

Model Visualization Techniques for a Social Network Model

Samantha Tyner*

Department of Statistics and Statistical Laboratory, Iowa State University
and

Heike Hofmann

Department of Statistics and Statistical Laboratory, Iowa State University

July 11, 2018

Abstract

Stochastic actor-oriented models, first introduced by Snijders (1996), are a type of statistical network model for dynamic social networks. Unlike other network models, SAOMs are not very well understood. We use model visualization techniques introduced in Wickham et al (2015) in order to make them a little less murky. The SAOMs are a prime example of a set of models that can benefit greatly from application of model visualization. With the help of static and dynamic visualizations, we bring the hidden model fitting processes into the foreground, eventually leading to a better understanding and higher accessibility of stochastic actor-oriented models for social network analysts.

Keywords: social network analysis, model visualization, dynamic networks, network visualization, network mapping, animation

*The authors gratefully acknowledge funding from the National Science Foundation Grant # DMS 1007697. All data collection has been conducted with approval from the Institutional Review Board IRB 10-347

Contents

1	Introduction	3
2	Networks and their Visualizations	5
2.1	Introduction to Network Structures	5
2.2	Visualizing Network Data	5
3	Defining SAOMs	7
3.1	Definitions, Terminology, and Notation	8
3.1.1	The Rate Function	8
3.1.2	The Objective Function	9
3.2	Fitting Models to Data	12
3.3	Example Data	12
4	Model Visualizations	16
4.1	The Models	17
4.2	View the model in the data space	18
4.3	Visualizing collections of models	22
4.3.1	Exploring the space of all possible models	23
4.3.2	Varying model settings	23
4.3.3	Fitting the same model to different data	23
4.3.4	Fitting the same model to the same data	25
4.4	Explore algorithms, not just end result	26
5	Discussion	31

1 Introduction

Social networks, such as collaboration networks between academic researchers or friendship networks in a school or university have been studied for decades. Statistical models such as exponential random graph models (ERGM) and latent space models (LSM) are often used when studying one observation of a network when trying to model its structure. Social networks can also be observed at many points in time, and ERGM or LSM may not be appropriate for modelling the changes because they do not model network change as time passes. When studying *dynamic networks*, networks observed at many time points, we need a model that allows for variation in the network over time. Models for dynamic social networks hold a great deal of potential because of how realistic they can be. Social networks do not form spontaneously, but rather they *evolve* over time as edges are formed and dissolved, and new nodes join the social structure. Modeling the underlying mechanisms that create network changes in time is very complex but also provides potential to uncover hidden truths.

To model dynamic social networks, we use stochastic actor-oriented models (SAOMs), introduced by Snijders (1996). These models are different from other network models because they allow us to add node level information into the model with the traditional network structure information. Adding node-level information into the model is a more intuitive approach to model changes in a social network. For example, we expect people with common interests to be more likely to form relationships, and SAOMs allow us to incorporate this information on shared interests in the modeling process.

Unlike other network models, SAOMs are not very well understood. They are relatively new, especially compared to the classic ERGMs, and they are not very tractable analytically. Likelihood functions quickly become very complex objects to analyze due to the dependency structure inherent in the data. Therefore, computational methods, such as Markov chain Monte Carlo (MCMC) are used to fit models. SAOMs are typically fit to dynamic social network data using a series of MCMC phases for finding method of moments (MoM) estimates of model parameters. In order to estimate the parameters of SAOMs, we use the software SIENA, and its R implementation `RSiena`, which was developed by Ripley et al. (2016a). This software is a considerable contribution to the field of social network

analysis, but the many simulations involved in parameter estimation are largely hidden from the software user. In order to better understand the model-fitting process of **RSiena**, we attempt to bring model fits and the fitting process to the foreground by visualizing the underlying methods and structures. Ultimately, we aim to help researchers working with the models better understand the structure of and results from these models.

To learn more about the SAOM fitting process, we use model visualization techniques (see Wickham et al. (2015)) to display the model in the data space, view collections of models instead of single models, and explore the algorithms fitting the SAOMs instead of studying only the final output. SAOMs are an excellent example of a family of models that can reap many benefits from the application of model visualization techniques. For instance, the models themselves include a continuous-time Markov chain (CTMC) that is completely hidden from the analyst in the model fitting process. Visualizing the CTMC can provide researchers with more insight into the underlying features of the model. In addition, SAOMs can include a great deal of parameters in the model structure, each of which is attached to a network statistic. These statistics are often somewhat, if not highly, correlated, which causes high correlation between the corresponding parameters in a SAOM. By visualizing collections of SAOMs, we gain a better understanding of these correlations and can find ways to account for their effects in the model. Furthermore, the estimation of the parameters in a SAOM rely on convergence checks based on simulations from the fitted model. These simulations are hidden and unsaved by default for computational efficiency. With the help of both static and dynamic visualizations, we bring the hidden model fitting processes into the foreground, eventually leading to a better understanding and higher accessibility of stochastic actor-oriented models for social network analysts.

The remainder of this paper is organized as follows: In Section 2, we introduce basic concepts of networks and network visualizations. In Section 3, we formally define the family of stochastic actor-oriented models for social network analysis. In Section 4, we combine concepts from Sections 2 and 3 in an application of the model-vis paradigm, and conclude with a discussion in Section 5.

2 Networks and their Visualizations

We provide a brief introduction to the structure of network data and common network visualization methods.

2.1 Introduction to Network Structures

Network data across fields have similar data structures. There are always units of observation and connections between those units. In a social network, the units of observations, called *nodes* or *actors*, may be people, while the connections, called *edges* or *ties*, are the relationships between people. Networks often change over time, like when new relationships are formed in a social network. The nodes and edges themselves can also have inherent variables of interest, e.g. the age, gender, and political affiliation of people in a social network and the type of relationship (friends, married, etc.).

These two network data structures pose unique problems to analysts, such as, “How does the strength of a tie between two nodes affect the overall structure of the network?” or “Do differences in node variables affect the formation of edges?” We propose to answer these questions and more through visual exploration of network data and models.

2.2 Visualizing Network Data

Network visualization, also called network mapping, is a prominent subfield of network analysis. Visualizing network data is uniquely difficult because of the structure of the data itself. Most data visualizations rely on well-defined axes inherited from the data, such as Cartesian coordinates or spatial locations. Network data, however, carry no such inherent structure.

There are two primary methods used to visualize networks that are very different from most traditional data visualizations. They are the node-link diagram and the adjacency matrix visualization (Knuth, 2013; Fekete, 2009). For example, consider a network with five nodes, $\{1, 2, 3, 4, 5\}$, connected by five directed edges: $\{2 \rightarrow 4, 3 \rightarrow 4, 1 \rightarrow 5, 3 \rightarrow 5, 5 \rightarrow 4\}$. This data is shown using the two visualization methods in Figure 1.

The first method, the node-link diagram, represents nodes with points in two dimensions

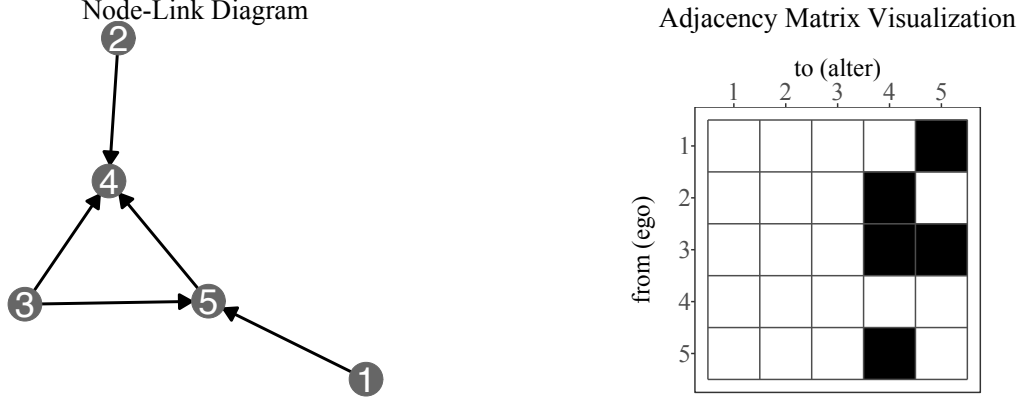


Figure 1: On the left, a node-link diagram of our directed toy network, with nodes placed using the Kamada-Kawai algorithm. On the right, the adjacency matrix visualization for that same network.

and then represents edges by connecting the points with lines. These lines can also have arrows on them indicating the direction of the edge for directed networks, as show in Figure 1. Because there is usually no natural placement of the points (the exception is nodes with spatial locations), a random placement of the points is used, then adjusted with a layout algorithm, of which there are many (Gibson et al., 2013).

Some commonly used layout algorithms, such as the Kamada-Kawai (KK) layout (Kamada and Kawai, 1989) and the Fruchterman-Reingold (FR) layout (Fruchterman and Reingold, 1991), are designed to mimic physical systems, drawing the graphs based on the “forces” connecting them. Other algorithms use multi-dimensional scaling or properties of the adjacency matrix (e.g. its eigenstructure), to place the nodes (Gibson et al., 2013). In Figure 1, we use the KK algorithm, and unless otherwise stated, all other node-link diagrams in this paper will use the KK layout.

The second method for network visualization uses the adjacency matrix of the network. The adjacency matrix of a network, \mathbf{A} is defined as follows: an entry A_{ij} of \mathbf{A} , for two nodes $i \neq j$ in the network is defined as

$$A_{ij} = \begin{cases} 1 & \text{if an edge exists } i \rightarrow j \\ 0 & \text{otherwise} \end{cases} \quad (1)$$

We only consider the presence or absence of an edge, but if the network has weighted edges, the entries in the adjacency matrix are the edge weights. An adjacency matrix visualization

for our toy example is also shown in Figure 1. This visualization shows the network as a grid, with each row and column representing a node. The grid space for edge $i \rightarrow j$ is filled in if $A_{ij} = 1$ and is empty if $A_{ij} = 0$.

Each visualization comes with its own advantages and disadvantages. For instance, paths between two nodes in a network are easier to determine with node-link diagrams than with adjacency matrix visualizations (Ghoniem et al., 2005). In node-link diagrams, node-level information can be incorporated into the visualization by coloring or changing the shape of the points, and edge-level information can be incorporated by coloring the lines, or changing their thickness or linetype. Incorporating a node-level variable into an adjacency matrix visualization is not as straightforward or simple, because this type of visualization features the edges. Adjacency matrix visualization can, however, be useful when the network is very complex, dense, or large (Ghoniem et al., 2005). Ultimately, there is no one “correct” way to visualize network information, and we will be using both the node-link and adjacency matrix visualization methods throughout this paper to explore social networks and stochastic actor-oriented models.

3 Defining SAOMs

A Stochastic Actor-Oriented Model (SAOM) is a model that incorporates all three data levels of dynamic networks: actor, tie, and temporal information. It models the change of a network in time, while accounting for changes in network structure due to actor-level covariates. This model was first introduced by Snijders in 1996 (Snijders, 1996). The two titular properties of SAOMs, stochasticity and actor-orientation, are key to understanding networks as they exist naturally. Most social networks, even holding constant the set of actors over time, are ever-changing as relationships decay or grow in seemingly random ways. Actors in social networks also have inherent properties that could affect how they change their role within the network, and existing ties may affect formation or dissolution of other ties.

3.1 Definitions, Terminology, and Notation

We use the term *dynamic network* to refer to a network, consisting of a fixed set of n nodes, that is changing over time, and is observed at M discrete time points, t_1, \dots, t_M with $t_1 \leq t_2 \leq \dots \leq t_M$. We denote the network observation at timepoint t_k by $x(t_k)$. The SAOM assumes that this longitudinal network of discrete observations is embedded within a continuous time Markov chain (CTMC), which we will denote $X(T)$. This process is almost entirely unobserved: we assume that the beginning of the process, $X(0)$, is equivalent to the first network observation $x(t_1)$, while the end of the process, $X(\infty)$, is equivalent to the last observation $x(t_M)$. Nearly all other steps in the chain are unseen, with the exception of $x(t_2), \dots, x(t_{M-1})$. Unlike the first and last observations of the network, these “in-between” observations do not have direct correspondence with steps in the continuous time Markov chain. Thus, the “in-between” observations are considered to be “snapshots” of the network at some point between two steps in the CTMC.

The CTMC process $X(T)$ is a series of single tie changes that happen according to some pre-defined rate function (Section 3.1.1), where one actor at a time is selected and it adds or removes one outgoing tie, or does nothing. Once an actor is chosen at random according to the rate function, it is “given” the chance to change a tie, and it tries to maximize its utility function (Section 3.1.2) based on the current and possible future states of the network.

3.1.1 The Rate Function

In general, each actor i in the network x may change its ties, x_{ij} , to other nodes $j \neq i$ according to the SAOM’s *rate function*, $\rho(x, \mathbf{z}, \boldsymbol{\alpha})$, where $\boldsymbol{\alpha}$ are the parameters in the function ρ , and x is the current network state, with covariates of interest \mathbf{z} . With this general formulation, it is possible that each node will have a different rate of change. We assume a simple rate function, $\rho(x, \mathbf{z}, \boldsymbol{\alpha}) = \alpha_m$ that is constant across all actors between time t_m and t_{m+1} . With this simple rate function, we have just one set of rate parameters in the overall model. In this simple model, the rate parameters dictate how often an actor i “gets an opportunity” to change one of its ties, x_{ij} , for $j \in \{1, \dots, n\}$ in the time period from t_m to t_{m+1} for $m = 1, \dots, M - 1$ (Note that when $j = i$, no change is made.) We also

assume that the actors i are conditionally independent given their ties, x_{i1}, \dots, x_{in} at the current network state. Let $\tau(i|x, m)$ be the wait time until actor i gets to the opportunity to change its current set of ties. For any time point, T , where $t_m \leq T < t_{m+1}$, the waiting time to the next change made by actor i is exponentially distributed with expected value α_m^{-1} . Then, we express this in Equation 2.

$$\tau(i|x, m)|x_{i1}(m), \dots, x_{in}(m) \stackrel{\text{iid}}{\sim} \text{Exp}(\alpha_m) \quad (2)$$

From Equation 2, we can derive the waiting time to the next change opportunity by *any* actor in the network, $\tau(x)$. The value $\tau(x)$ is also exponentially distributed with expected value $(n\alpha_m)^{-1}$, where $n\alpha_m$ is the rate at which any tie change occurs. The estimation of this parameter in **RSiena** is simple: the method of moments is used to estimate the rate with the statistic

$$C = \sum_i \sum_j |x_{ij}(t_{m+1}) - x_{ij}(t_m)| \quad (3)$$

which is the total number of changes from observation at time t_m to the observation at time t_{m+1} .

3.1.2 The Objective Function

Because of the conditional independence assumptions given in Equation 2, we can consider the objective function for each node separately, as only one tie from one node is changing at a time in the CTMC. The node i , which is the node that is given the opportunity to change at the current time point, is called the *ego* node. It has the potential to interact with all other nodes in the network, $j \neq i$. These nodes j , are referred to as *alter* nodes, and do not change any of their ties when i may change. For the ego node i in the current network state x , its *objective function*, which it tries to maximize, is written as

$$f_i(\boldsymbol{\beta}, x) = \sum_k \beta_k s_{ik}(x, \mathbf{Z}), \quad (4)$$

for $x \in \mathcal{X}$, the space of all possible directed networks with the n nodes, and \mathbf{Z} , the matrix of covariates. The vector $\boldsymbol{\beta}$ contains the parameters of the model with corresponding network and covariate statistics, $s_{ik}(x, \mathbf{Z})$, for $k = 1, \dots, K$. To increase the value of f_i , i will

destroy one tie where $x_{ij} = 1$, create one tie where $x_{ij} = 0$, or make no change if any changes result in lower values of f_i .

According to Snijders (2001, p. 371), there should be at least two parameters included in the model: β_1 for the outdegree of a node, and β_2 for the number of reciprocal ties held by a node. (These effects are also used in ERGMs.) The outdegree represents the propensity of nodes with a lot of outgoing ties to form more outgoing ties (the "rich get richer" effect), and the reciprocity parameter measures the tendency of outgoing ties to be returned within a network. The statistics corresponding to these two parameters, $s_{i1}(x)$ and $s_{i2}(x)$ are given in Figure 1. In the **RSiena** software, there are over 80 possible β parameters to add to the model. The formulas for the corresponding statistics for all effects are provided in Ripley et al. (2017).

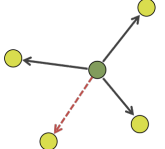

The β parameters are either structural or covariate parameters. The structural parameters, such as the outdegree and reciprocity parameters, correspond to statistics that are only functions of the current network state, x . They model underlying mechanisms of network change, answering questions such as, "How does the existing network structure influence change in the network?" The covariate parameters are functions of x and additional node-level covariates of interest, \mathbf{Z} . A table of some possible structural and covariate parameters and their corresponding statistics is given in Table 1.

The objective function also defines the probability that actor i , when it is the ego node, chooses to change the tie to actor j , $p_{ij}(\beta, x, \mathbf{Z})$. Let $x(i \rightsquigarrow j)$ denote the network identical to x with the exception of tie x_{ij} . It has changed to $1 - x_{ij}$. The probability that the tie x_{ij} changes is defined as:

$$p_{ij}(\beta, x, \mathbf{Z}) = \frac{\exp \{f_i(\beta, x(i \rightsquigarrow j), \mathbf{Z})\}}{\sum_{h \neq i} \exp \{f_i(\beta, x(i \rightsquigarrow h), \mathbf{Z})\}} \quad (5)$$

When $i = j$, the numerator represents the exponential of the value of the objective function when evaluated at the current network state. When the value of the objective function is high at the current state, the probability of not making a change is also high. In the CTMC, when actor i may make a change, it chooses which tie x_{i1}, \dots, x_{in} to change at random according to the probabilities $p_{ij}(\beta, x, \mathbf{Z})$. The objective function and the resulting values of p_{ij} are combined with the rate function to fully describe the CTMC that is used to model

Structural Effects

Name	Statistic	Figure
outdegree	$s_{i1}(x) = \sum_j x_{ij}$	
reciprocity	$s_{i2}(x) = \sum_j x_{ij}x_{ji}$	

Covariate Effects

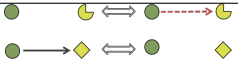
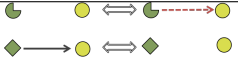
Name	Statistic	Figure
covariate-alter	$s_{i4}(x) = \sum_j x_{ij}z_j$	
covariate-ego	$s_{i5}(x) = z_i \sum_j x_{ij}$	

Table 1: Examples of effects included in a SAOM. The dark nodes in the Figures are the ego nodes, and all others are alters. The dotted lines are ties the ego node is en(dis)couraged to make when the parameter corresponding to each effect is positive (negative). Node shapes represent levels of the covariate z .

network change in a SAOM. For more on CTMCs, see Yin and Zhang (2010). We explore these probabilities further in Section 4.4

3.2 Fitting Models to Data

To fit a SAOM to dynamic network data, we apply the **RSiena** software, which uses simulation methods to estimate parameter values using either MoM or maximum likelihood (ML) estimation (Ripley et al., 2016a). We chose to use MoM estimation, so we describe that fitting process here, and more information on ML estimation can be found in Snijders (2016).

The underlying SIENA software uses a Robbins-Monro algorithm (see Robbins and Monro (1951)) to estimate the solution of the moment equation

$$E_{\theta}S = s_{obs}$$

where $\theta = (\alpha, \beta)$ is the vector of rate and objective function parameters, and s_{obs} is the observed vector of model statistics. The full SIENA MoM estimation algorithm operates in three phases, as described in Ripley et al. (2017); Snijders (2016). The first phase performs initial estimation of the score functions for use in the Robbins-Monro procedure for MoM estimation. The second phase carries out the Robbins-Monro algorithm and obtains estimates of the parameter values through iterative updates and simulation from the CTMC at iterative parameter values. The third phase uses the parameter vector estimated in phase two to estimate the score functions and covariance matrix of the vector of parameter estimates and carries out convergence checks.

In each of the the first two phases of the algorithm, the procedure uses “microsteps” that are simulated from the model as it exists in its current state in order to update either the score functions or the parameter estimates. These simulated microsteps are observed instances of the CTMC that is the backbone of the SAOM. In Section 4, we further explore these phases in the SIENA method-of-moments algorithm through visualization, bringing them out of their “black box” and into the light.

3.3 Example Data

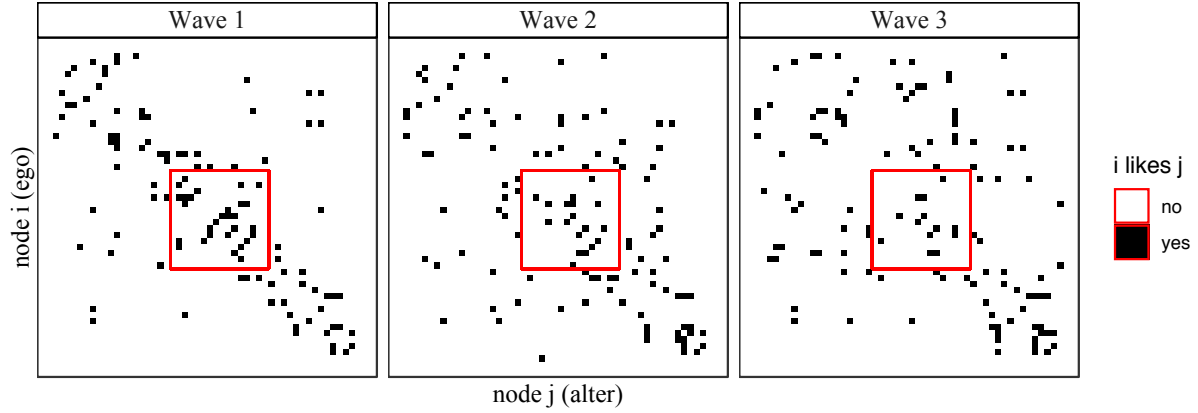


Figure 2: A visualization of the adjacency matrices of the three waves of network observations in the “Teenage Friends and Lifestyle Study” data. The subset we will be using is outlined in red.

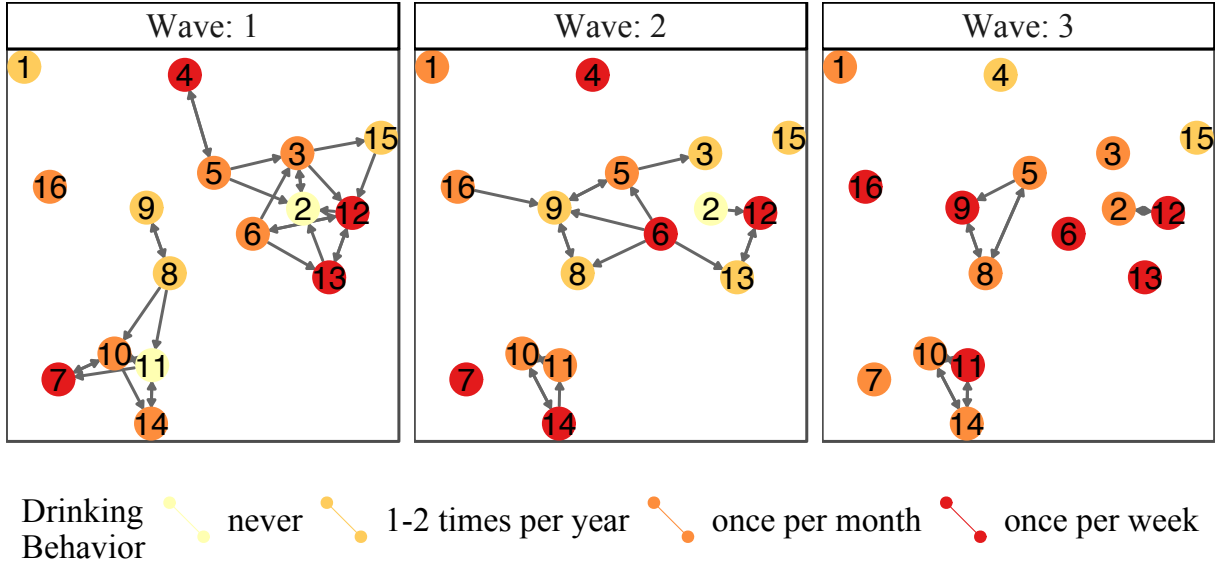


Figure 3: The smaller friendship network data we will be modelling throughout the paper. The nodes change color as their drinking behavior changes, and the network becomes less densely connected over time. These are the mechanisms we hope to capture with SAOMs.

To guide our visual exploration of SAOMs, we use two example data sources. The first is a subset of the 50 actor dataset from the “Teenage Friends and Lifestyle Study” that is provided on the *RSiena* webpage. These data come from Michell and Amos (1997), and we chose to only work with a subset of the data to make node-link diagrams easier to see and to make any changes in the network more noticeable. In Figure 2, we show the

adjacency matrix visualization of all three observations of this network, with the subset we selected for analysis outlined in red. This subset contains 16 actors, their ties and their drinking behavior for three timepoints. The node-link visualization of the data is provided in Figure 3. For model fitting, we condition on wave 1 and estimate the parameters of the models for the second and third waves. The actor-level categorical covariate, drinking behavior, has four values: (1) does not drink, (2) drinks once or twice a year, (3) drinks once a month, and (4) drinks once a week. In Figure 3, the nodes are colored according to the drinking behavior of that student. Over time, we can see that the students tend to drink more and become increasingly isolated into smaller groups. An analysis of this type of data with a SAOM should capture these dynamics in a way that allows the researcher to draw conclusions about the nature of the network and behavioral forces at play.

The second data example we use is a collaboration network in the United States Senate during the 111th through 114th Congresses. These sessions of congress correspond to the years of Barack Obama’s presidency, from 2009-2016. (Details of how this data can be downloaded are provided by Francois Briatte at <https://github.com/briatte/congress>). In this network, ties are directed from senator i to senator j when senator i cosponsors the bill that senator j authored. There are hundreds of ties between senators when they are connected in this way, so we simplify the network by computing a single value for each pair of senators called the *weighted propensity to cosponsor* (WPC). This value is defined in Gross et al. (2008) as

$$WPC_{ij} = \frac{\sum_{k=1}^{n_j} \frac{Y_{ij(k)}}{c_{j(k)}}}{\sum_{k=1}^{n_j} \frac{1}{c_{j(k)}}} \quad (6)$$

where n_j is the number of bills in a congressional session authored by senator j , $c_{j(k)}$ is the number of cosponsors on senator j ’s k^{th} bill, where $k \in \{1, \dots, n_j\}$, and $Y_{ij(k)}$ is a binary variable that is 1 if senator i cosponsored senator j ’s k^{th} bill, and is 0 otherwise. This measure ranges in value from 0 to 1, where $WPC_{ij} = 1$ if senator i is a cosponsor on every one of senator j ’s bills and $WPC_{ij} = 0$ if senator i is never a cosponsor any of senator j ’s bills.

Because we require binary edges for SAOMs, we focus only on very strong collaborations.

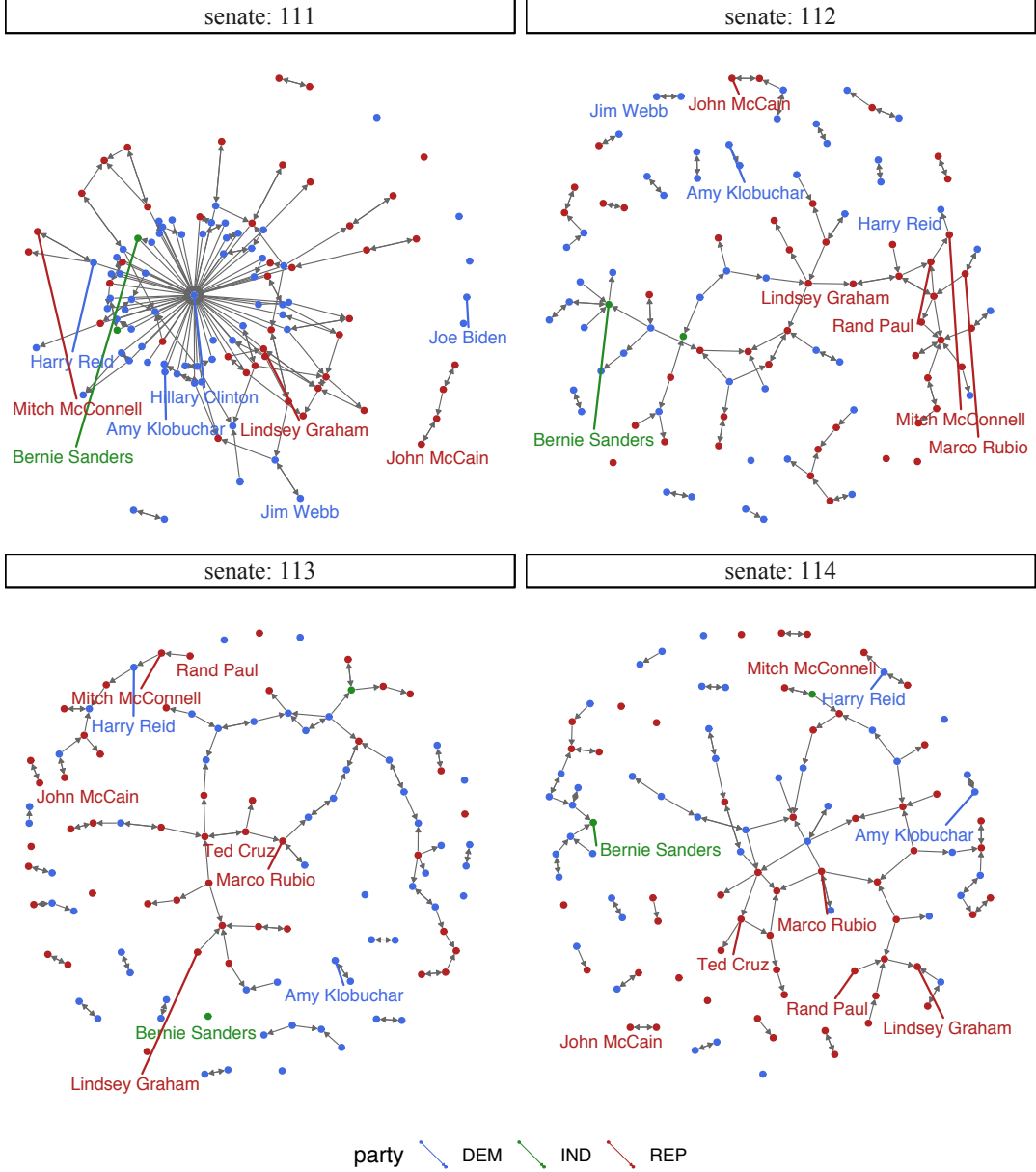


Figure 4: The collaboration network in the four senates during the Obama years, 2009-2016. Edges are shown only if the WPC between two senators is greater than 0.25. We use the FR layout algorithm here.

For our senate collaboration networks, x , edges are defined as

$$x_{ij} = \begin{cases} 1 & \text{if } WPC_{ij} > 0.25 \\ 0 & \text{if } WPC_{ij} \leq 0.25. \end{cases} \quad (7)$$

The node-link diagram for the four senates during the Obama administration are shown

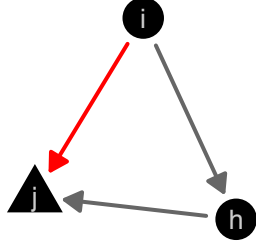
in Figure 4. We can see that Senate 111 is much more densely connected than the other three, which have one large, sparsely connected component with a few smaller connected groups throughout. Some prominent names are shown to demonstrate their place in the network.

We use these two example newtorks to demonstrate our model visualization methods for SAOMs in section 4

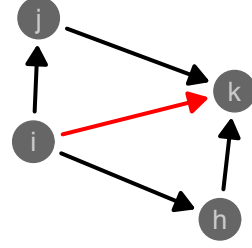
4 Model Visualizations

Every good data analysis includes both numerical and visual summaries of the data, so why restrict model description and diagnostics to numerical summaries? The concept of model visualization was developed to complement traditional model diagnostic tools such as R^2 values and residual plots (Wickham et al., 2015). When performing analyses, there are three different types of “model”: the model family, the model form, and the fitted model. The latter is primarily what one thinks of first when considering a model in a data analysis, where a specified model is fit to data, and parameter estimates are reported. The *model form* describes the the model *before* the fitting process, defining which parameters are in the model within the context of the larger model family. Finally, the *model family* is the broadest description of the model. This is the type of model that you wish to fit to the data, and is chosen based on the problem, data, and knowledge at hand.

The model family, the model form, and the fitted model can each be visualized according to the three principles of model visualization: we can view the model in the data space, visualize collections of models, and explore the process of fitting the model, not just the end result. Since we have already decided on our model family, SAOMs, we shift our focus to the fitted model and the model form. Specifically, we want to learn more about how the *model form* we choose affects the *fitted model* by using our example data sets and our visualization toolbox. We begin by introducing the five models that we fit to our example data. We then use the five models to guide our visual explorations of SAOMs under the three principles of model visualization.



(a) Realization of a JTT, where i is the ego, j is the alter, and h is the intermediary. The covariate is represented by the shape of the nodes.



(b) Realization of a N22 between actors i and k .

Figure 5: The additional network effects included in our models fit to the friends data. On the left, a JTT and on the right, a N22 between i and k .

4.1 The Models

We first consider the 16 actor subset of the teenage friends and lifestyle data show in Figure 3. To this data, we fit three different SAOMs. Each SAOM used a simple rate function, α_m , and an objective function with two or three parameters. The first model, M1, contains the absolute minimum number of parameters in the objective function $f_i(x)$:

$$f_i(x)^{M1} = \beta_1 s_{i1} + \beta_2 s_{i2}, \quad (8)$$

where s_{i1} is the density network statistic and s_{i2} is the reciprocity network statistic for actor i at the current network state x . The second and third models, M2 and M3, contain one additional parameter each in the objective function which were determined by a Wald-type test provided in the **RSiena** software to be significant, with p -values less than 0.05 (Ripley et al., 2016b). The M2 model contains an actor-level covariate parameter, and the M3 model contains an additional structural effect in the objective function.

$$f_i(x)^{M2} = \beta_1 s_{i1} + \beta_2 s_{i2} + \beta_3 s_{i3} \quad (9)$$

$$f_i(x)^{M3} = \beta_1 s_{i1} + \beta_2 s_{i2} + \beta_4 s_{i4}, \quad (10)$$

where $s_{i3} = \sum_{j \neq h} x_{ij} x_{ih} x_{hj} \mathbb{I}(z_i = z_h \neq z_j)$, and $s_{i4} = |\{j : x_{ij} = 0, \sum_h x_{ih} x_{hj} \geq 2\}|$. These statistics are known as the *number of jumping transitive triplets* (JTT) and the

number of doubly achieved distances two effect (N22), respectively. The first statistic emphasizes triad relationships that are formed between actors from different covariate groups, while the other emphasizes indirect ties between actors. The covariate groups are determined by the student’s drinking behavior. These additional effects are shown in Figure 5a and Figure 5b.

It is often difficult to know for certain how to interpret a fitted value of a parameter. We can make educated guesses based on the definition of the effect and the sign of the fitted value, but a direct interpretation is not always possible. By graphically exploring these models, we aim to understand their effects, their interpretations, and the model fitting process better.

In Section 4.3.3, we also fit models M1, M2, and M3 to the senate collaboration data for comparison. To fit M2 to the senate data, we use the number of bills authored by each senator as the node covariate for the jumping transitive triplet variable.

4.2 View the model in the data space

The first way we hope to better understand SAOMs is by viewing the model(s) in the data space. In Wickham et al., they chose to define the *data space* as “the region over which we can reliably make inferences, usually a hypercube containing the data” (Wickham et al., 2015, p. 206). But what does this definition mean for network models? We define the data space as the combined data structures of the network: the node, edge, and time information.

The node, edge, and time data can be visualized together in various ways, and one tool that can bring the node, edge, and time data spaces together is the R package `geomnet` (Tyner and Hofmann, 2016). Different visual features in the node-link diagram can be tied to the underlying node or edge data. The color, size, and shape of the points can be used to represent variables in the node data, while the color, linewidth, and linetype of the lines between points can be used to represent the edge variables. To view temporal changes, we can view the network at different timepoints side-by-side to see the evolution. Pulling all of this information together with `geomnet` allows the entire data space to be viewed at once.

To demonstrate, we use `geomnet` to visualize the connections in the 111th United States Senate at two different points: when Hillary Clinton was in the senate, and after she left to

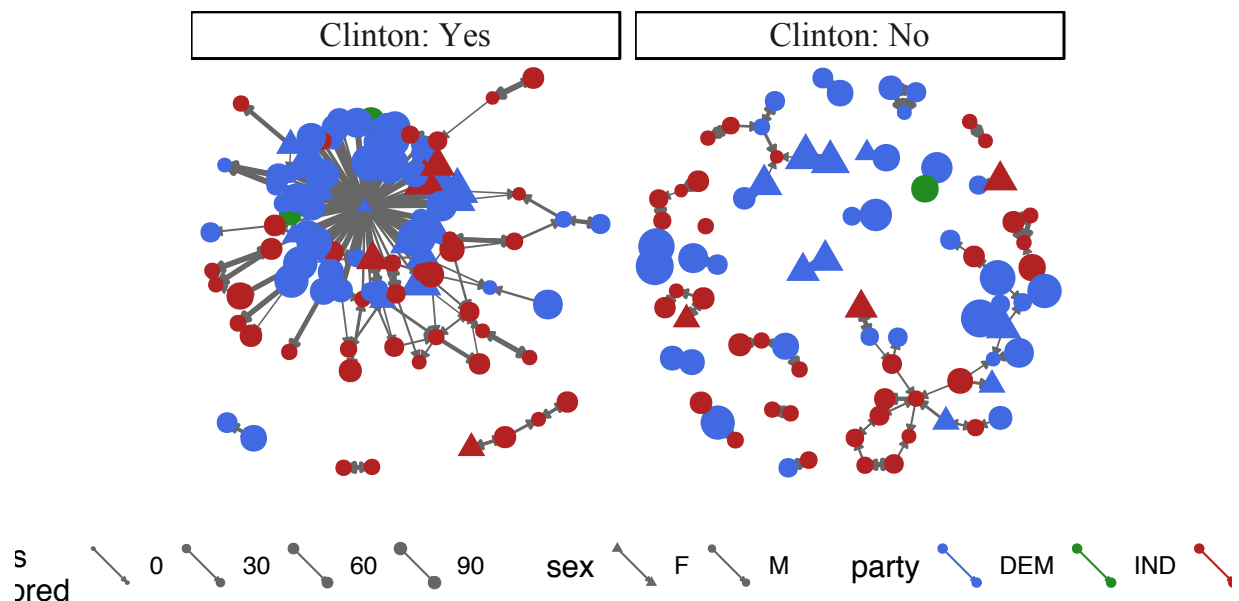


Figure 6: The 111th Senate at two times: while Clinton was in the senate in 2009 (on the left) and after she left (on the right). We map sex, party, and bills authored to the shape, color, and size of the nodes, respectively. We also map the WPC , to the edge linewidth.

become Secretary of State. Clinton was only in the 111th senate for 17 days, from January 3, 2009, to January 20, 2009, when she was in the middle of her second term as senator from New York. In that time, she authored two bills and was a cosponsor on 17 other bills. There are many Democratic senators who cosponsored both of her bills, giving their edges a WPC of 1. So with Clinton included in the node-link diagram, the senate looks much more collaborative than it does without her. We then map the size of the node to the number of bills authored by the senator, the shape to sex, color to party. Bills, sex, and party are all potential covariates in a SAOM. In addition, we visualize the strength of the tie by mapping the linewidth of the edge to the WPC value between the two senators. In this single visualization, we have viewed node information, edge information, and time. We will use `geomnet` many ways to view the model in the data space.

Another way to view the model in the data space is through simulation from the model. No one network simulated from a SAOM is going to look like the data or represent the model, so we might want to look at an “average network” or “expected network” value. We frequently rely on averages and expected values in data analyses, but network models, especially those as complex as SAOMs, lack an expected network value measure. We could

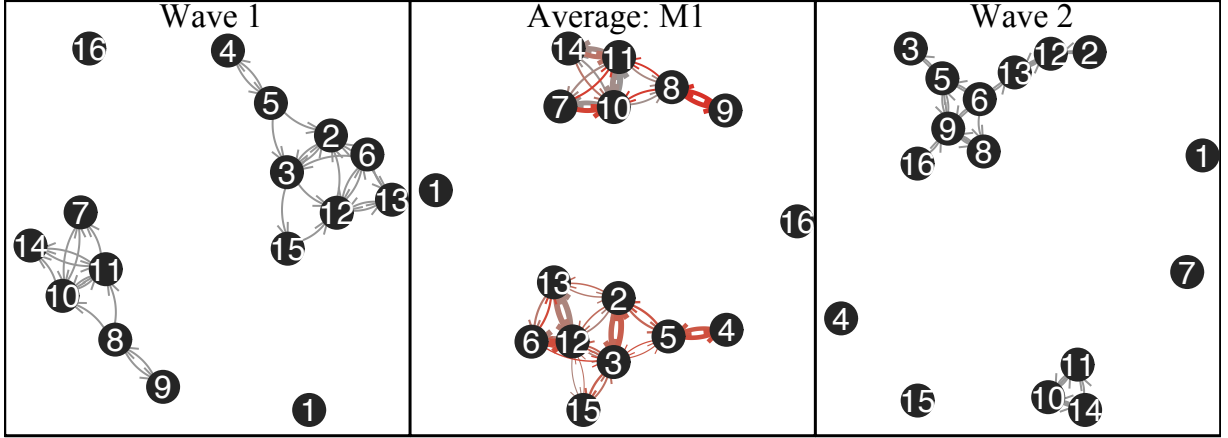


Figure 7: On the left, the first wave of observed data that is conditioned on in the model. On the right, the second wave of observed data. In the middle, a summary network from the first model fit to the data. This summary network represents 1,000 simulations of wave 2 using the values from the simple fitted model M1.

talk about expected values of parameters, but the parameters can be hard to interpret. There is no defined expected value of an simulation from a network model, though there are with most other model simulations. How then, can we arrive at an “average” network? We answer this question through visualization.

For network data, one way we view an “average” network is through a sory of summary network drawn using the traditional node-link diagram. In Figure 7, we show an *average network* created with 1,000 simulations of the second wave of the network from Model 1. To make this average network, we first simulated 1,000 wave 2 and wave 3 observations of our small friendship example data from model M1, for which parameters had previously been estimated. We then combine the 1,000 simulated instances of wave 2, and count up the number of times each edge appears in a network simulation. Then, we combine these 1,000 networks into a single network with edgeweight equal to the proportion of time that edge appears in our 1,000 simulations. This weighted edgelist is the network we draw in Figure 7. An edge is only drawn in the average network if it appears in at least 51 of the 1000 simulations, with edges that appear with greater frequency emphasized by thicker linewidths and a darker color. On either side of the average network in Figure 7, we show

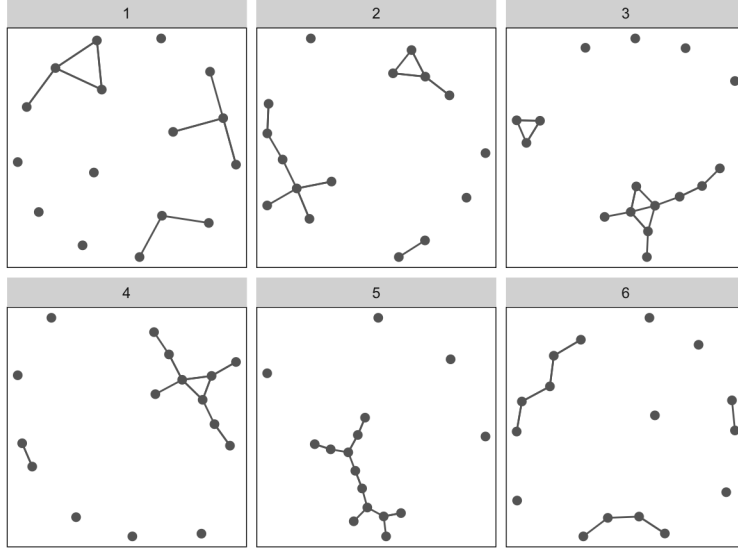


Figure 8: A small lineup of node-link diagrams showing the second wave of our small friendship network among five networks simulated from model M1.

the actual data, wave 1 on the left, and wave 2 on the right. We can see that the structure of the average network is much more similar to the first wave than to the second wave. However, the simulations are supposed to represent the second wave of data on the right of Figure 7. This is an indication that the simple model, M1, is doing a very poor job of capturing the change mechanism from the first to the second wave of observation. The average network can thus be used to help determine model goodness-of-fit. Because the the average network looks more like the first wave than the second wave, we can use the visualization in Figure 7 as evidence of poor model fit.

Another potential goodness-of-fit visualization that places the fitted model in the node and edge data space is a lineup like those proposed in Buja et al. (2009). A *lineup* “asks the witness to identify the plot of the real data from among a set of decoys, the null plots, under the veil of ignorance” (Buja et al., 2009, p. 4369). It can be thought of like a police lineup, where the “suspect” is in a lineup among several innocent similar looking people, and if the witness picks the suspect out of the lineup, that is evidence the suspect is guilty.

In data and model visualization, the “suspect” is a plot of the true data, while the “filler” is composed of several plots of “mock data”, simulated from a hypothesized model. If the true data stands out among the simulated data, that is taken as evidence against the hypothesised model. If, however, the true data is difficult to identify among the simulated

data, that is taken as evidence in favor of the hypothesized model.

The data visualizations examined in previous applications such as Hofmann et al. (2012) are less complex than a node-link network diagram. Typically, the lineup viewers have to pick out the most different plot, which is hard for network data. As an example, consider the network lineup shown in Figure 8. In this small network lineup, the second wave of the small friendship network is shown among five simulated networks from model M1 using parameter values estimated from the data. It seems possible to argue for any one of the six plots in Figure 8 as most different. So, we suggest guiding participants to look at the overall structure of the graphs to determine which has the most or least connected or complex structure. In a future paper, we will use the lineup protocol to help better understand SAOMs by allowing us to view the model in the data space.

4.3 Visualizing collections of models

The second method of model visualization we use is visualizing collections of models. There are many possible ways to collect SAO models together, so for the SAOMs, we decided that there were four ways to create collections of models that would give us the most insight:

1. exploring the space of all possible models;
2. varying model settings;
3. fitting the same model form to different data;
4. fitting the same model to the same data many times

We chose these four collections because they each explore something different about SAOMs. The first considers the many parameters to include in a SAOM. The second collection shows how those many parameters affect the parameter values of the fitted models. The third looks at how the same model behaves when fit to different data. Finally, the results from fitting the same model to the same data may lead to different parameter estimates, so we want to see how the parameter estimates can vary.

4.3.1 Exploring the space of all possible models

The **RSiena** manual contains over eighty effects to include in a SAOM. In order to select parameters to include in the models for our example data, we searched through the possible effects available to model given the data structure to find *significant* effects. We tested for significance using the Wald-type tests built into **RSiena** for one-at-a-time effects testing. We start with the outdegree and reciprocity measures as the foundation of the models we fit, then add one effect, fit the model, test the additional effect for significance, and repeat for all possible parameters to add to the model. We performed this procedure for both the small friendship and the senate collaboration data. A visualization of the significant effects for the two example data sets are shown in Figure 14 in the Appendix.

4.3.2 Varying model settings

We have varied model settings already by choosing models M1, M2, M3 to fit to our small friendship network data set. In Section 4.3.4, we fit these models to the data 1,000 times, and in this section, we explore simulations from these three models given the mean values of from the 1,000 fitted parameter values as the parameters in our models. From each of these three models using the means of parameter estimates as our fixed parameter values, we simulated 1,000 observations from each of the three models. From these simulations, we create visualizations that represents an average network using the same method described in Section 4.2, shown in Figure 15 in the Appendix.

4.3.3 Fitting the same model to different data

In addition to fitting M1, M2, and M3 to the friendship data 1,000 times, we also fit them to the senate data 100 times. The means and standard deviations of the parameter estimates for each combination of model and data are given in Table 2, while the density plots of each parameter in the model for each data set is given in Figure 9.

Looking at Figure 9 and Table 2, we see a few patterns in the estimates from both models. First, the table and the density plots demonstrate the same relationship between the outdegree parameter, β_1 , and the reciprocity parameter, β_2 . In both data sets and across all three models, the estimates of β_1 are all negative and hover between -5 and -3, while the

	Friendship Data			Senate Data		
	M1	M2	M3	M1	M2	M3
α_1	4.660 (0.059)	5.176 (0.068)	4.712 (0.060)	3.344 (0.016)	3.349 (0.016)	3.340 (0.016)
α_2	1.930 (0.026)	2.017 (0.028)	1.979 (0.027)	2.480 (0.017)	2.487 (0.015)	2.483 (0.014)
α_3	—	—	—	2.221 (0.017)	2.227 (0.017)	2.224 (0.016)
β_1	-3.597 (0.033)	-4.104 (0.038)	-3.589 (0.035)	-4.979 (0.027)	-4.993 (0.025)	-4.987 (0.021)
β_2	4.149 (0.050)	4.277 (0.052)	4.230 (0.050)	4.954 (0.046)	4.974 (0.040)	4.970 (0.035)
β_3	—	3.209 (0.053)	—	—	-1.175 (0.789)	—
β_4	—	—	-7.582 (1.746)	—	—	-1.048 (0.486)

Table 2: The means (std. dev.) of parameter values estimated from repeated fittings of $M1, M2, M3$ to the two example data sets.

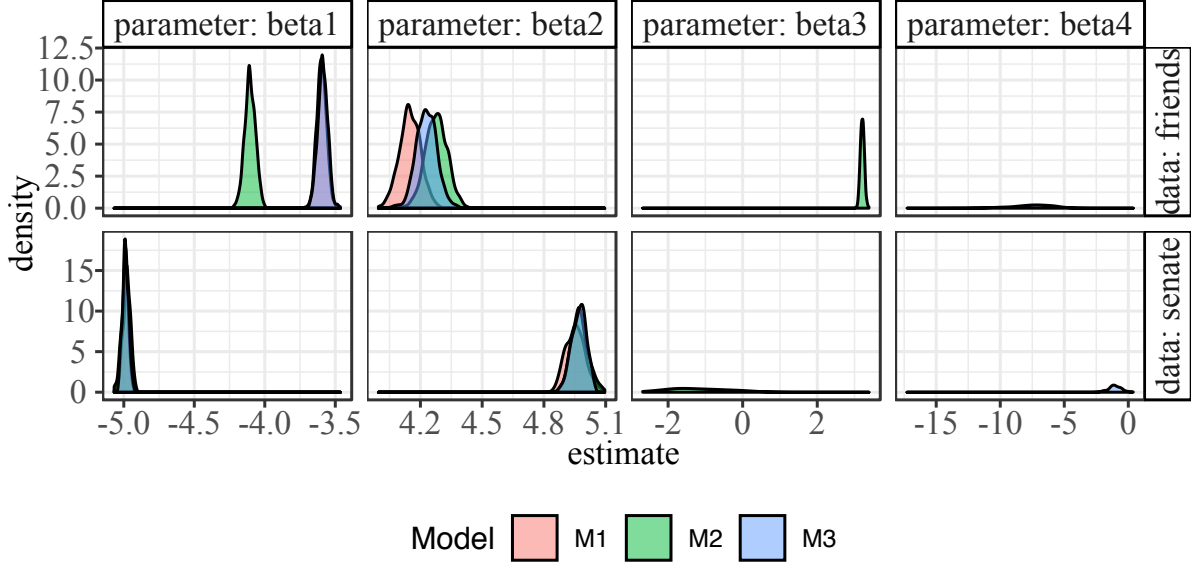


Figure 9: Density plots of objective function parameter estimates from repeatedly fitting models $M1, M2$, and $M3$ to the example data. Outdegree and reciprocity have the same inverse relationship for both data sets. For the friendship data, the inclusion of β_3 has strong effect on the estimates of the other two parameters, but not for the senate data.

estimates of β_2 are all positive and hover between four and five. This suggests that in both data sets, nodes are *encouraged* to form outgoing ties that are reciprocated and *discouraged* from forming ties that are not. Actors in these networks want reciprocated relationships: the students want to have close mutual friendships, and senators want mutual support for

their bills. We explore the relationship between β_1 and β_2 further in Section 4.3.4.

The inclusion of β_3 , the JTT parameter, for the friendship data had a noticeable effect on the other parameters in the model. This is not true in the senate data. Looking at the estimates of β_4 , we see that the estimates for the senate data are near zero, suggesting that this effect, which considers indirect ties, is not important for the senate data. It is, however, much stronger in the friendship data, suggesting that indirect ties are discouraged from forming: teenage girls want to have direct friendships. This indirect relationship variable does not impact the senate collaboration structure, but it does affect teenage friendship structure.

4.3.4 Fitting the same model to the same data

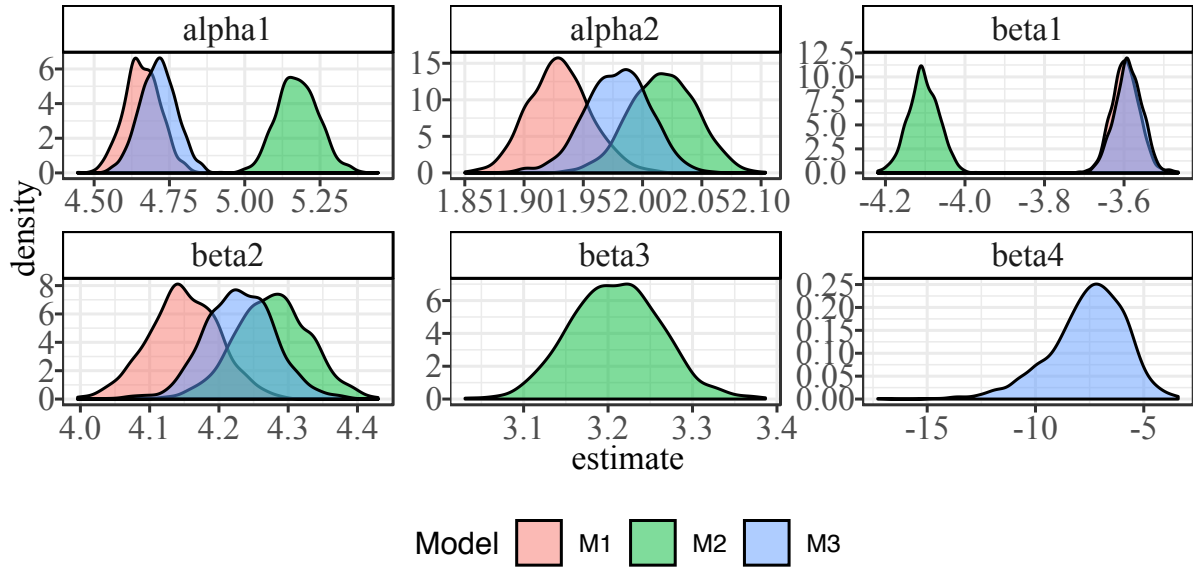


Figure 10: Distribution of fitted parameter values for our three SAOMs. The inclusion of β_3 or β_4 clearly has an effect on the distribution of the rate parameters, α_1 and α_2 .

After fitting models M1, M2, and M3 to the friendship network 1,000 times each, we examine the distribution of the fitted values, which are shown in Figure 10. We can see from these distributions that the inclusion of the jumping transitive triplet parameter, β_3 is obviously affecting the distributions of the other four parameters included in all models, α_1 , α_2 , β_1 , and β_2 . When β_3 is included, its estimate is positive, meaning that friend-

ships between two girls with different drinking behaviors tend to form when there is an intermediary who is already friends with the two girls. The inclusion of this parameter leads to increases in the rate parameters’ estimates, suggesting that encouraging the transitive triplet behavior means that the girls would also change friends more frequently. The outegree parameter, β_1 decreases when β_3 is included, while the reciprocity parameter, β_2 increases. This implies the girls in the data prefer to form closer friend groups, as indicated by reciprocated ties and jumping transitive triplet formation, as opposed to being popular and having many friends. Having many friends who do not reciprocate is more strongly discouraged by M2 than in the other models. In comparison with models M1 and M3, model M2 typically has higher estimates of the rate parameter, meaning that the inclusion of the covariate statistic in the model leads to higher estimates of the number of times, on average, a node gets to change its ties. It is not clear, however, that the addition of a parameter to the objective function *should* effect the estimation of the rate parameters. The strong correlations between the estimates of the rate parameters and of the objective function parameters are shown in Figure 16 in the Appendix.

4.4 Explore algorithms, not just end result

The last principle of model visualization we use is exploring the process of fitting the model, instead of just focusing on the end result. This principle is perhaps the most important for SAOMs because the model fitting process in **RSiena** involves several simulation steps that are hidden from the user. Hiding the MCMC steps is practical and efficient if a researcher is primarily interested in fitting one model to a set of longitudinal network data, obtaining parameter estimates, and drawing conclusions or making predictions. We are more interested in *how* the models are fit, so we extracted and explored the different steps of that process instead of allowing them stay hidden.

A key component of each step of the SIENA method of moments algorithm is the “microstep” process. A series of microsteps is obtained by simulating from the model in its current state, $x(t_m)$ with current parameter values $\theta_0 = \{\alpha_{1_0}, \dots, \alpha_{m-1_0}, \beta_{1_0}, \dots, \beta_{K_0}\}$, to the next state, $x(t_{m+1})$. This microstep process stops when the simulated network has achieved the same number of differences, C , from $x(t_m)$ as $x(t_{m+1})$, where C is defined

in Equation 3.

This simulation process follows the steps of the continuous-time Markov chain. Each tie change in the CTMC is referred to as one “microstep”. At each microstep, an “ego node” is selected to make a change, and the chosen ego node randomly makes one change in its ties according to the probabilities, $\{p_{ij} : i \neq j \in \{1, \dots, n\}\}$ defined in Equation 5, determined by its objective function. The options for change are (1) removing a current tie, (2) adding a new tie, or (3) making no change at all. Between two network observations $x(t_m)$ and $x(t_{m+1})$, there can be dozens, hundreds, or even thousands of microsteps, depending on the size of the network and the number of changes between two network observations. We want to view these in-between steps in order to better understand the behavior of the underlying continuous-time Markov chain.

The first vizualization we present here is an animation of the simulated microsteps that form the transition steps of the CTMC from wave 1 to wave 2 of the small friendship network example shown in Figure 3 when fitting model M1. Movies similar to this animation were used to visualize the changes of dynamic networks in Moody et al. (2005). When each ego node is selected in a microstep, it is emphasized in the animation, then the associated edge either appears or disappears. If there are no changes at a particular microstep, no changes are seen. Some frames of the animations are shown in Figure 17 in the Appendix, and the full movie can be viewed at <https://vimeo.com/240089108>.

In the network animation, we see the possible steps of the unobserved CTMC process that is underlying the SAOM fit to the data. We see each part of the model come into play. First, we see the rate at which the nodes are selected to change. Then, we see the result of the actor maximizing its objective function by either deleting or adding a node. In addition, the layout of the nodes changes as edges are removed or added, which gives us a better sense of how the overall network structure changes with these individual tie changes.

We next use animation to view the changing structure of the adjacency matrix the microsteps. The adjacency matrices for the three waves of friendship data as shown in Figure 3 are ordered by node id. There are 16 nodes in the data, numbered 1-16, and that order is used on the x and y axes for the matrix visualization. Viewing the adjacency

matrices with this arbitrary ordering does not provide much information to the viewer about the underlying structure of the network. This lack of perceived structure would be exacerbated in an animation, so we adjust the ordering so that the viewer can better perceive the structure of the network. This process is known as matrix seriation (Liiv, 2010).

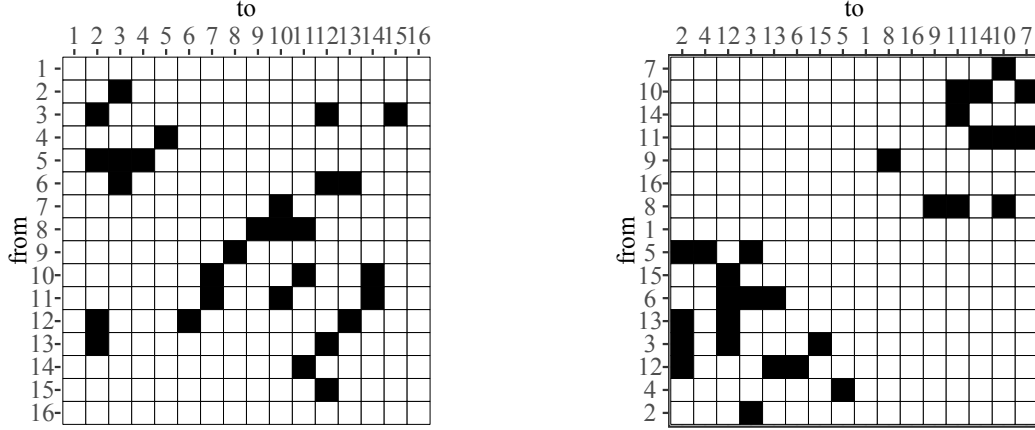


Figure 11: On the left, the starting friendship network represented in adjacency matrix form, ordered by vertex id. On the right, the same adjacency matrix is presented after ordering the vertices by one repetition of the microstep simulation process from wave one to wave two.

To reorder the vertices for the matrix visualization, we first constructed a cumulative adjacency matrix, \mathbf{A}^{cum} , for the series of microsteps simulating the network from $x(t_m)$ to $x(t_{m+1})$. A single entry in the cumulative adjacency matrix, \mathbf{A}_{ij}^{cum} , is the total number of times the edge from node i to node j appears in the network from the initial observation, $x(t_m) \equiv X(0)$ to the final result of the last microstep, $X(R)$, where R is the total number of microsteps taken:

$$\mathbf{A}_{ij}^{cum} = \sum_{r=0}^R X_{ij}(r).$$

We then performed a principal component analysis (PCA) on \mathbf{A}^{cum} , and used the values of the first principal component to order the vertices on the x and y axes for the adjacency matrix animation. For one such series of microsteps simulated by **RSiena**, we present the adjacency matrix ordered by the (arbitrary) vertex id alongside the seriated adjacency matrix using the first principal component loading on the cumulative adjacency matrix, \mathbf{A}^{cum} , in Figure 11.

Using PCA on \mathbf{A}^{cum} to order the rows and columns of the adjacency matrix visualization clearly shows the two distinct connected components in the first wave of the network, which are difficult to find in the arbitrarily ordered visualization. We also use the PCA seriated layout to fix the layout in the animation of one of the microstep process simulations. This animation, some frames of which are shown in Figure 18 of the Appendix is very simple: a square appears or disappears in the animation as that edge appears or disappears in the microstep process. Through this animation, which can be viewed at <https://vimeo.com/240092677>, we can see edges appearing, and then later on disappearing. These in-between steps are not shown when we look at the network at our discrete observation points, so by viewing this animation we can gain a better understanding of the underlying dynamics of this model.

We also attempt to better understand the microstep process by visualizing the observed transition probabilities for the first microstep in the process. These probabilities are defined in Equation 5. We only do the first step of many because the **RSiena** transition probabilities for any two edges i, j after the first step are only directly comparable for identical microsteps due to the conditioning on the current network state in the model. Thus we have 1,000 transition probabilities to examine: one transition probability for the first microstep taken for each of the simulations.

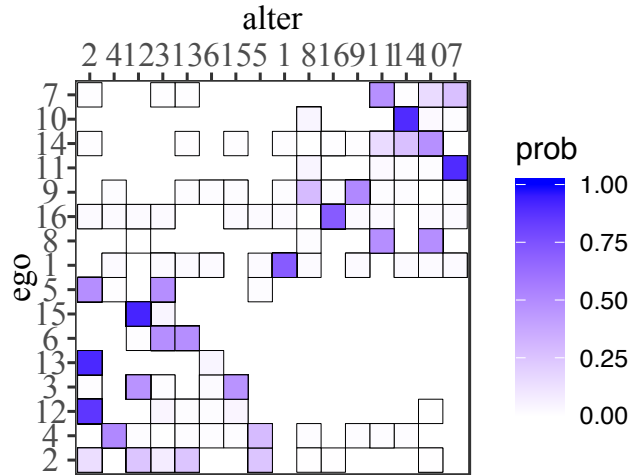


Figure 12: A heatmap showing the empirical transition probabilities for the first microstep in 1,000 simulations. The acting ego node is on the y-axis, and the alter node is on the x-axis. There were many ties with empirical probability zero.

In Figure 12, we build on the concept of the ordered adjacency matrix of Figure 11. This heatmap shows the transition probabilities of all ties that are changed in the first microstep of the 1,000 simulations. The heatmap is noticeably sparse: of the $16^2 = 256$ possible steps for the CTMC to take, only 103, or about 40%, are taken in the 1,000 simulated chains. This leaves a very large area of our network space, \mathcal{X} , completely unexplored by the SAOM model fitting process.

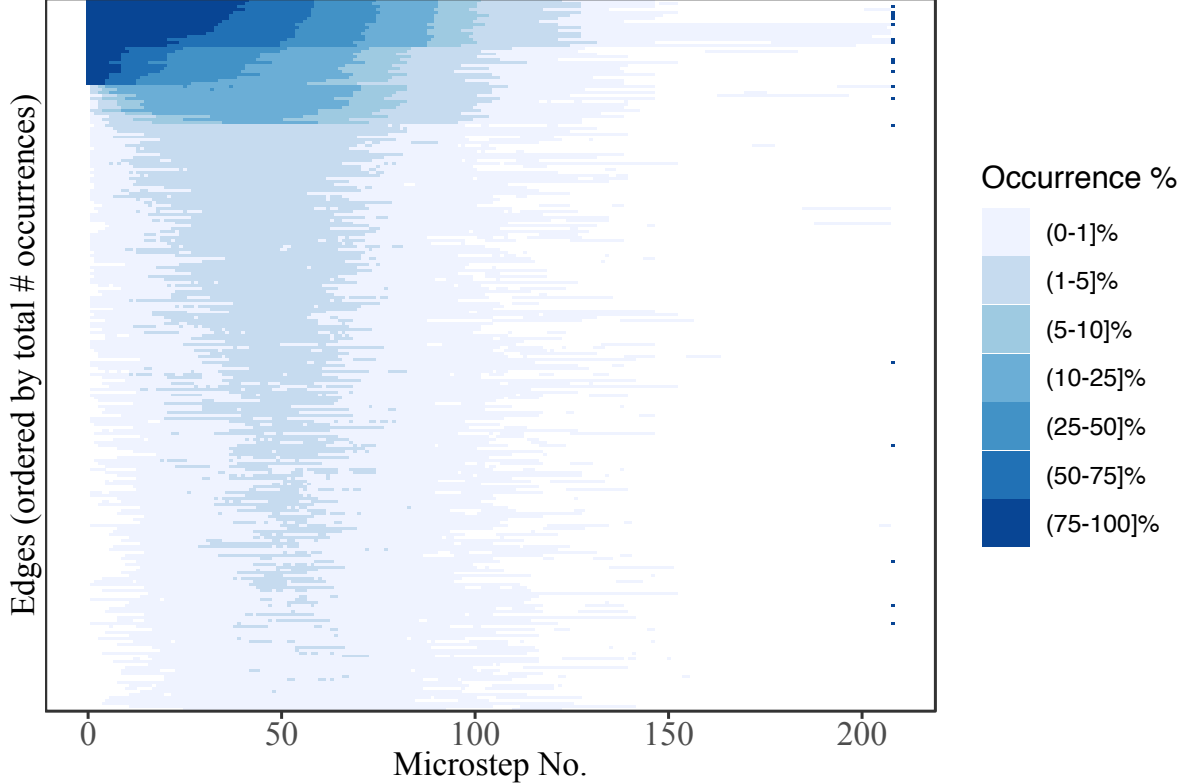


Figure 13: Visualizing all microsteps taken in 1,000 simulations from the model M1. The occurrence percent is split up into groups to correspond with its distribution: only about 10% of the edges appear more than 10% of the time in the 1,000 simulations, while about 60% appear less than 1% of the time. The first wave network is shown at microstep 0, and the second wave of the network is shown as the last microstep for comparison. We see that it is rare for a microstep process to last longer than 150 steps, and also that the edges that appear past the 150th step tend to be in either the first wave or the second wave.

Finally, we combine 1,000 simulations from model M1 into a visualization that displays the entire microstep process for all simulations in Figure 13. To make this visualization, we

first assign each possible edge an edge ID number so that we can keep track of it throughout all the microsteps and all the simulations. Then, we count up the total number of times each edge appears in the microstep process in each of the 1,000 simulations for use as an ordering variable later. We also count up the number of times an edge occurs in each microstep number in the 1,000 simulations. Since the number of microsteps in the process varies, the number of times an edge occurs decreases as the microstep number increases. Next, we compute a proportion, which we call the occurrence percentage, which is the number of times the edge occurred in a microstep divided by 1,000. Finally, we visualize all this information together in Figure 13. In this plot, all possible edges are shown, and we see that every one of the $16 \times 15 = 240$ possible edges in the network occurs at some point in the simulation process. We also see, however, that the process struggles to focus in on the edges in the second wave of the data. Ideally, we would like to see more occurrences of the edges which appear in the second wave of data. But, about half of the edges in wave two are in the bottom half when ordered by number of occurrences, meaning they do not appear as much as they would if the model was truly excellent at capturing the mechanisms of tie change in the network. This solidifies what we found in Figure 12: the model M1 and the SAOM fitting process do not explore the data space enough to adequately capture the network change mechanism.

5 Discussion

We have used novel visualization methods in order to better understand the family of models known as stochastic actor-oriented models for social network data. By looking at the underlying algorithms, visualizing collections of these models, and viewing the model in the data space, we have been able to gain knowledge and appreciation for these complicated models and everything that goes into them.

We have only just begun to scratch the surface of these complicated and multi-layered models for social networks. The **RSiena** software is incredibly powerful, and can fit a whole slew of much more flexible stochastic actor-oriented models than we have examined here. If a researcher thinks the network structure or an actor covariate effects the rate of change of the network, there is a way to incorporate that belief into the rate function of the SAOM.

More than one actor-level covariate can be included in the model, and way more than three parameters can be included in the objective function itself. In addition, **RSiena** allows the user to tell it which parameters lead to tie creation, and which parameters lead to tie endowment, or dissolution. We have used “evaluation” parameters, which assume that creation and endowment are equal (Ripley et al., 2017). Finally, SAOMs and **RSiena** are able to also model behavior change of the actors in the network, which again is a capability we did not explore here.

Appendix: Additional visualizations

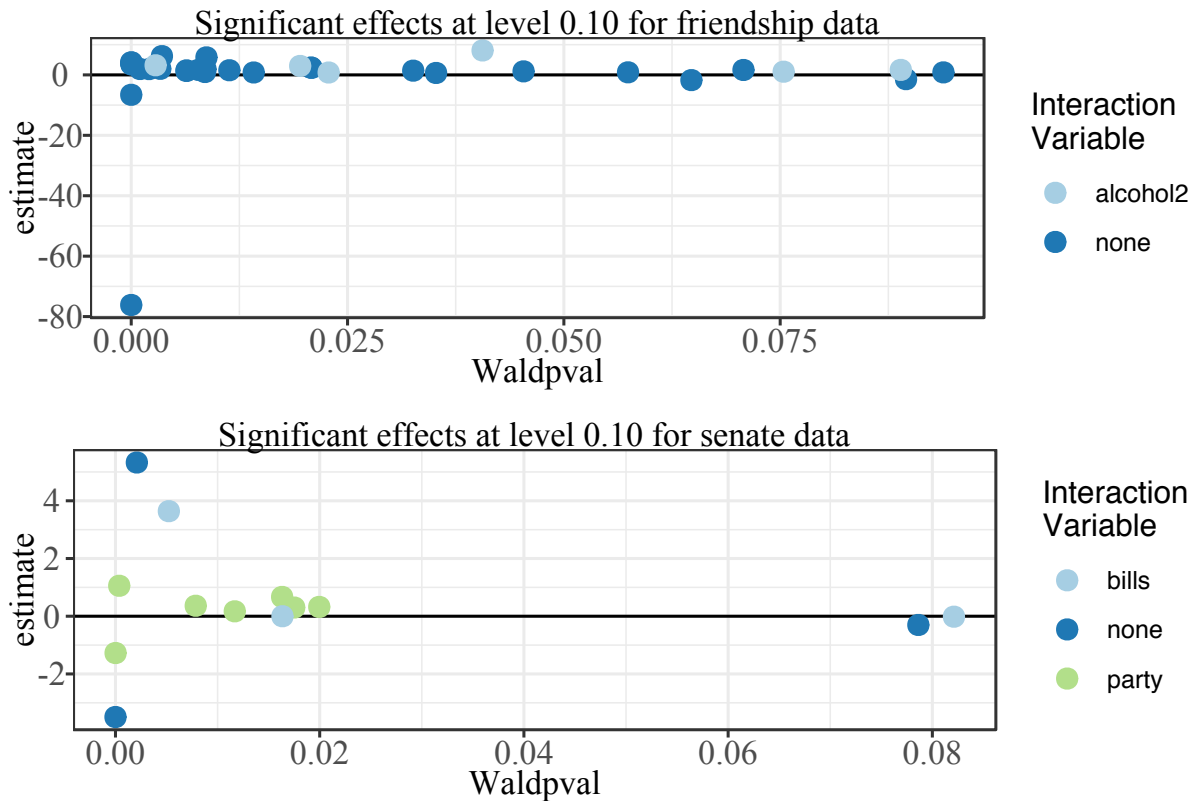


Figure 14: From Section efsec:allpossible. Significant effects for the two data sets, at a significance level of 0.10 or lower as calculated by the Wald-type test available in the SIENA software.

In Figure 14, we see in both the friendship data and the senate data results that most of the significant effects have absolute value less than ten. In addition, the p -values for the effects from the friendship data are more spread out than the p -values for the senate

data, which are concentrated at about 0.02 or less. This may suggest that larger data sets tend to result generally in smaller p -values, just like a larger sample size results in smaller p -values in a t -test.

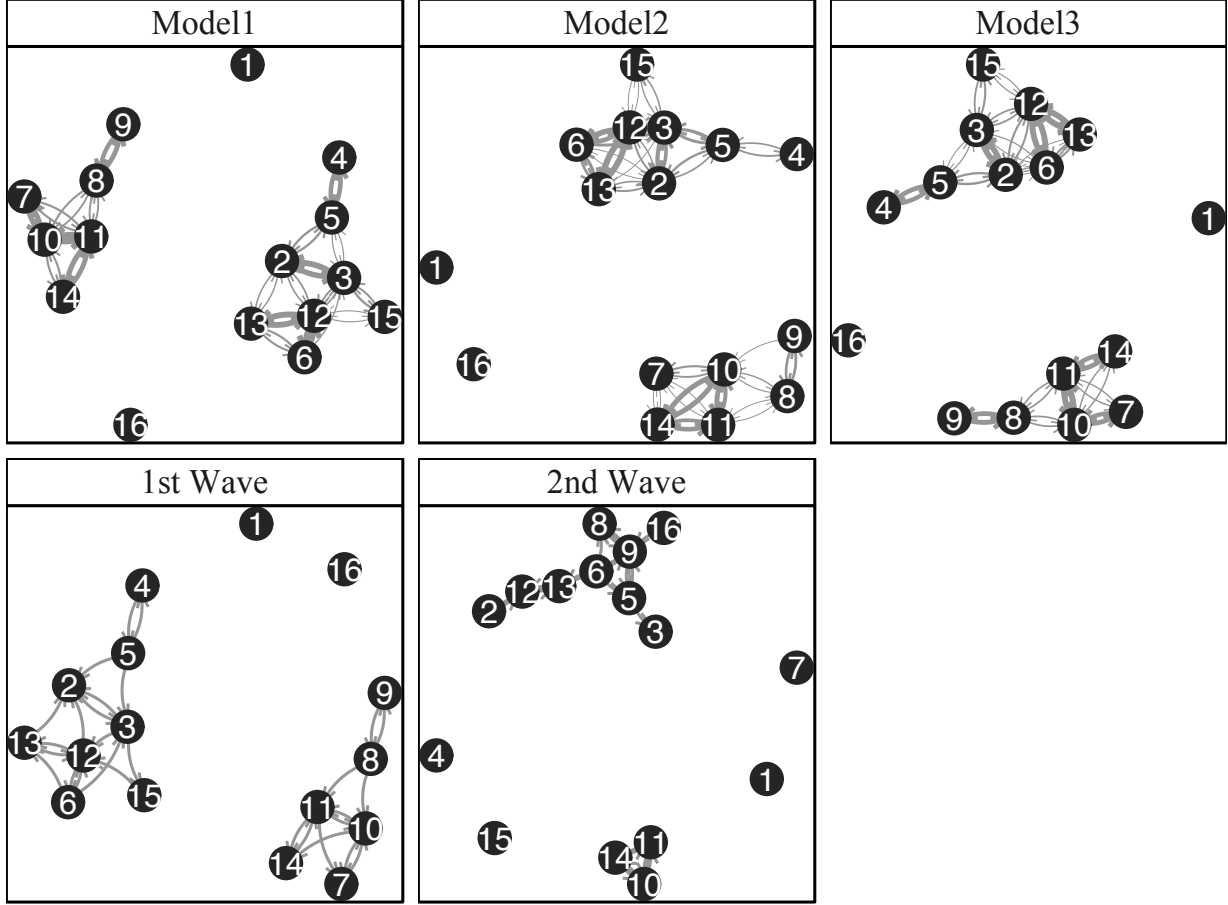


Figure 15: The node-link diagrams from the three "average" networks that we calculated are in the top row, and the true wave 1 and wave 2 data are shown in the bottom row above. There is some difference between the three models, but overall, these three models cannot capture the structure in the true second wave of data.

To create the average network visualization shown in Figure 15, we follow the same procedure as in Section 4.2, counting occurrences of each possible edge in the simulations, resulting in a summary network with weighted edges representing the number of times an edge appeared in the simulated wave 2 when simulating from the SAOM 1,000 times. As

in Figure 7, edges only appear in the average networks if they appear more than 5% of the time in the simulations. In Figure 15, we show the “average” network from the three models we fit and the first and second waves of data. Comparing the three averages to waves 1 and 2, we see that they have very similar structure to wave 1. Model 2, which included the transitive triplet parameter, seems to have created a larger connected component overall than models 1 and 3. In particular, if we look at the group of nodes $\{10, 11, 14\}$, we see they are very strongly connected within the three average networks, and they are completely separate from the other nodes in the true wave 2. None of the three average networks show node 16 gaining ties as it does in wave two, nor do they show nodes 4 and 7 becoming isolated. In Model 2, however, the ties to node 7 appear much weaker than in Model 1 or Model 2, suggesting that of the three, Model 2 may be the best fit for our data.

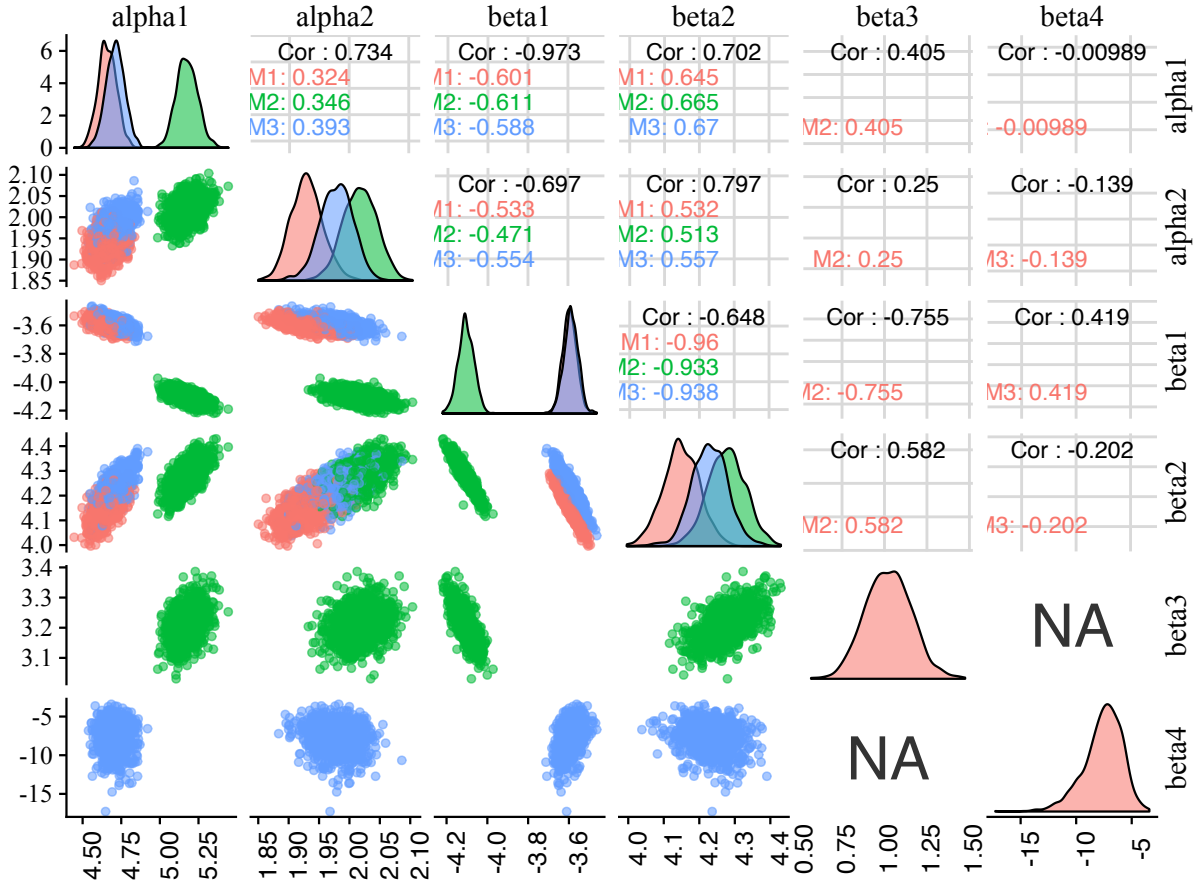


Figure 16: A matrix of plots demonstrating the strong correlations between parameter estimate in our SAOMs. The strongest correlation within each model is between β_1 and β_2 .

In Figure 16, we examine correlations between each of pair of parameters within each model and overall. The strongest correlation within each model is between β_1 and β_2 , with absolute value of correlation between those two parameter values greater than 0.90 in all three models. The β_1 parameter is also highly correlated with the β_3 parameter within model M2, but it is not as highly correlated with the β_4 parameter in model M3. It might therefore be advisable to consider only models that either allow β_1 , or β_2 . Looking at the high correlation with α , we might switch to a model without β_1 .

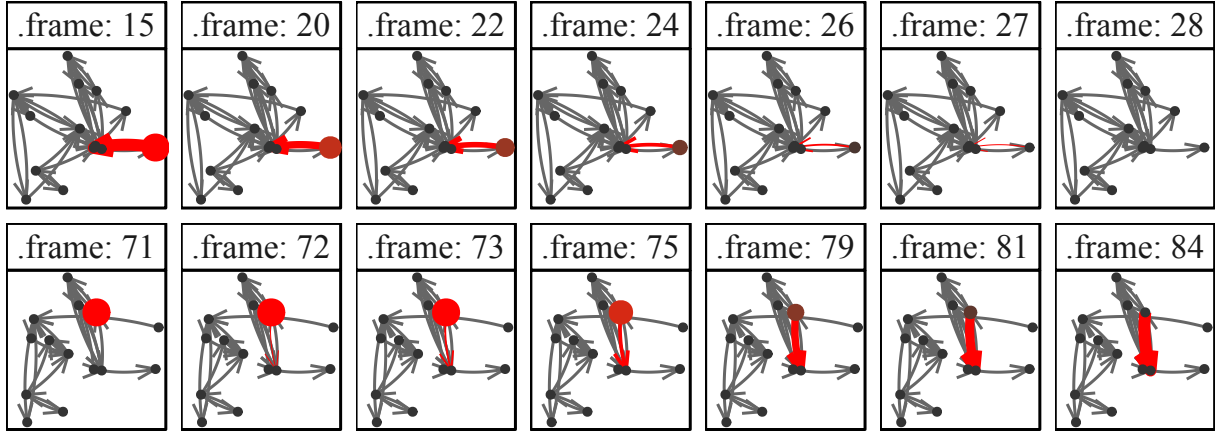


Figure 17: A selection of images in the microstep animation. The selected edges and nodes are emphasized by changing the size and the color, then when edges are removed, they fade out, shrinking in size, while the nodes change color and shrink to blend in with the other nodes.

The top row of Figure 17 shows an edge being removed, and the bottom row shows one being added. In both cases, the ego node that is acting changes color from black to red, and they also increase greatly in size. In the case of an edge being removed, in the top row, the edge that currently exists is emphasized with the same color and size change that the node gets, and as the animation proceeds the edge shrinks to nothing, as the ego node shrinks and changes color back to its original black. If an edge is being added, as in the bottom row of the figure, the ego node's appearance changes in the same way as when the edge is being removed, while the edge appears colored red from nothing, and grows to a large size, then changes color and size to match the rest of the edges, while the node shrinks and changes color to match the other nodes.

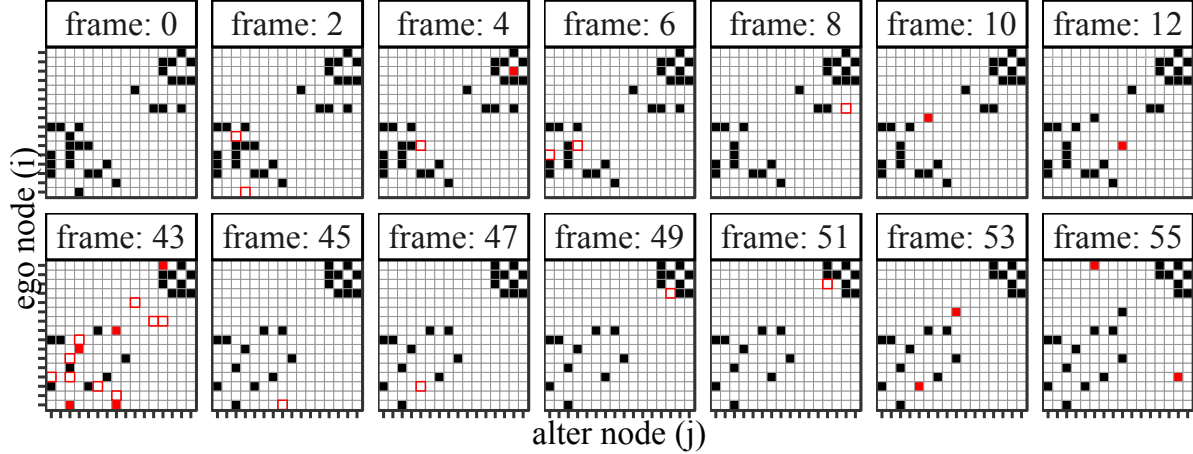


Figure 18: A selection of frames from the adjacency matrix visualization animation for one series of microsteps. (Ego and alter node labels are removed to declutter the graph.) At the beginning of the animation, shown in the top row, there are two clearly connected components: one in the top left corner, and one in the bottom right corner. By the end, the component in the top left has spread out, while the bottom right component has shrunk, but remains closely connected.

References

- Buja, A., Cook, D., Hofmann, H., Lawrence, M., Lee, E., Swayne, D., and Wickham, H. (2009), “Statistical Inference for Exploratory Data Analysis and Model Diagnostics,” *Royal Society Philosophical Transactions A*, 367, 4361–4383.
- Fekete, J.-D. (2009), “Visualizing Networks using Adjacency Matrices: Progresses and Challenges,” in *11th IEEE International Conference on Computer-Aided Design and Computer Graphics*, pp. 636–638.
- Fruchterman, T. M. and Reingold, E. M. (1991), “Graph Drawing by Force-Directed Placement,” *Software: Practice and Experience*, 21, 1129–1164.
- Ghoniem, M., Fekete, J.-D., and Castagliola, P. (2005), “On the readability of graphs using node-link and matrix-based representations: a controlled experiment and statistical analysis,” *Information Visualization*, 4, 114, copyright - Palgrave Macmillan Ltd 2005; Document feature - charts; graphs; tables; references; equations; Last updated - 2012-01-28.

- Gibson, H., Faith, J., and Vickers, P. (2013), “A survey of two-dimensional graph layout techniques for information visualisation,” *Information Visualization*, 12, 324–357, copyright - SAGE Publications Jul 2013; Document feature - Tables; ; Last updated - 2013-08-05.
- Gross, J. H., Kirkland, J. H., and Shalizi, C. R. (2008), “Cosponsorship in the U.S. Senate: A Multilevel Two-Mode Approach to Detecting Subtle Social Predictors of Legislative Support,” *Unpublished Manuscript*.
- Hofmann, H., Follett, L., Majumder, M., and Cook, D. (2012), “Graphical tests for power comparison of competing designs,” *Visualization and Computer Graphics, IEEE Transactions on*, 18, 2441–2448.
- Kamada, T. and Kawai, S. (1989), “An Algorithm for Drawing General Undirected Graphs,” *Information Processing Letters*, 31, 7–15.
- Knuth, D. E. (2013), *Combinatorics: Ancient and Modern*, Oxford University Press, chap. Two thousand years of combinatorics.
- Liiv, I. (2010), “Seriation and Matrix Reordering Methods: An Historical Overview,” *Statistical Analysis and Data Mining*, 3, 70–91.
- Michell, L. and Amos, A. (1997), “Girls, pecking order and smoking,” *Social Science & Medicine*, 44, 1861 – 1869.
- Moody, J., McFarland, D., and Bender-deMoll, S. (2005), “Dynamic Network Visualization,” *American Journal of Sociology*, 110, 12061241.
- Ripley, R., Boitmanis, K., Snijders, T. A., and Schoenenberger, F. (2016a), *RSiena: Siena - Simulation Investigation for Empirical Network Analysis*, R package version 1.1-304/r304.
- (2016b), *RSienaTest: Siena - Simulation Investigation for Empirical Network Analysis*, R package version 1.1-294.

- Ripley, R. M., Snijders, T. A., Boda, Z., Vrs, A., and Preciado, P. (2017), *Manual for RSiena*, University of Oxford: Department of Statistics; Nuffield College; University of Groningen: Department of Sociology, https://www.stats.ox.ac.uk/~snijders/siena/RSiena_Manual.pdf.
- Robbins, H. and Monro, S. (1951), “A stochastic approximation method,” *The Annals of Mathematical Statistics*, 22, 400–407.
- Schloerke, B., Crowley, J., Cook, D., Hofmann, H., Wickham, H., Briatte, F., Marbach, M., and Thoen, E. (2016), *GGally: Extension to ggplot2*, R package version 1.3.0.
- Snijders, T. A. (2016), *Siena Algorithms*, University of Oxford: Department of Statistics, https://www.stats.ox.ac.uk/~snijders/siena/Siena_algorithms.pdf.
- Snijders, T. A. B. (1996), “Stochastic actor-oriented models for network change,” *Journal of Mathematical Sociology*, 21, 149–172.
- (2001), “The Statistical Evaluation of Social Network Dynamics,” *Sociological Methodology*, 31, 361–395.
- Tyner, S. and Hofmann, H. (2016), *geomnet: Network Visualization in the 'ggplot2' Framework*, r package version 0.2.0.9001.
- Wickham, H., Cook, D., and Hofmann, H. (2015), “Visualizing statistical models: Removing the blindfold,” *Statistical Analysis and Data Mining: The ASA Data Science Journal*, 8, 203–225.
- Yin, G. G. and Zhang, Q. (2010), *Continuous-Time Markov Chains and Applications: A Two-Time-Scale Approach*, New York: Springer, 2nd ed., ISBN 978-1-4614-4345-2.